Dependence of Tryptophan Emission Wavelength on Conformation in Cyclic Hexapeptides

Chia-Pin Pan,[†] Patrik R. Callis,*[,‡] and Mary D. Barkley*[,†]

Department of Chemistry, Case Western Reserve University, 10900 Euclid Avenue, Cleveland, Ohio 44106, and Department of Chemistry and Biochemistry, Montana State University, Bozeman, Montana 59717

Received: October 26, 2005; In Final Form: January 25, 2006

The wavelength of maximum emission of tryptophan depends on the local electrostatic environment of the indole chromophore. The time-resolved emission spectra of seven rigid cyclic hexapeptides containing a single tryptophan residue were measured. The emission maxima of the three decay-associated spectra for the seven peptides ranged from 341 to 359 nm, suggesting that different tryptophan rotamers have different emission maxima even in the case of solvent-exposed tryptophans. This conclusion is supported by quantum mechanical/molecular dynamics simulations of the six canonical side chain rotamers of tryptophan in solvated hexapeptides. The calculated range of emission maxima for the tryptophan rotamers of the seven peptides is 344−365 nm. The precision of the wavelength calculations and the peptide, water, and charged side chain contributions to the spectral shifts are examined. The results indicate that the emission maxima of decay-associated spectra can aid in the assignment of fluorescence lifetimes to tryptophan rotamers.

1. Introduction

Tryptophan (Trp, W) fluorescence is highly sensitive to the local environment of the indole chromophore. Individual tryptophans in peptides and proteins almost always have complicated decay kinetics that depend on emission wavelength.[1] The fluorescence decay data give good fits to multiexponential functions. The excited-state heterogeneity is generally attributed to ground-state heterogeneity, resulting from multiple tryptophan side chain rotamers or multiple protein microstates that do not interconvert on the fluorescence time scale. Because of the ubiquitous red-shifting of the decay-associated emission spectra (DAS) with increasing lifetime, explanations involving solvent relaxation and other excited-state reactions have also been proposed.[2−4] The standard rotamer model postulates that the local environment of the indole ring differs among rotamers, thereby causing the different fluorescence lifetimes and emission spectra.[5,6] Assigning rotamer conformations to lifetimes and emission spectra is a key step in analyzing the effects of protein environment on tryptophan fluorescence. The current strategy of assignment is based on qualitative or quantitative comparison of ground-state rotamer populations with fluorescence decay amplitudes. The former have been determined by NMR spectroscopy,[7,8] molecular modeling,[9,10] and X-ray crystallography.[11,12] The accuracy of NMR-derived rotamer populations and decay amplitudes generally limits assignment to a major species, which exists in both ground and excited states. However, even this correlation may be confounded by lack of a major species in one or both states, inconsistency between rotamer populations and decay amplitudes, or unresolved rotamers or lifetime components, in addition to variations from the standard rotamer model. Thus, it would be useful to have additional physical properties for correlating ground- and excited-state species.

We have developed a model system consisting of seven cyclic hexapeptides to test various hypotheses about tryptophan photophysics.[8,13] The cyclic peptides each have a single tryptophan at one of five positions in the sequence, a single backbone conformation, and three lifetime components. Comparison of NMR-derived rotamer populations and decay amplitudes assigned the major χ_1 rotamer to the major lifetime component in six of the seven peptides. Five lifetimes ranging from 2.7 to 5.5 ns were assigned to a $\chi_1 = -60°$ rotamer; one 0.5 ns lifetime was assigned to a $\chi_1 = 180°$ rotamer. The NMR experiments showed no evidence for a major χ_2 rotamer. The emission maxima of the seven peptides varied about 5 nm from 350 to 355 nm. Furthermore, the centers of gravity λ_{cg} of the DAS of the three lifetime components covered a 5−11 nm range within a given peptide, with four peptides showing the common correlation of wavelength and lifetime. These spectral shifts elicited two questions. Does the wavelength dependence of the DAS arise from differences among rotamers in the local environment of the indole ring? If so, is it possible to use λ_{max} of DAS to correlate ground- and excited-state species?

The wavelength of maximum emission λ_{max} of tryptophan depends on electrostatic environment.[14,15] The increase in permanent dipole moment for the transition from ground to the ^1L_a state, the emitting state in polar environments including virtually all proteins,[16] is about 6 D.[17] Moreover, the resultant direction of the excited-state dipole is nearly parallel to that of the ground state.[16] Theoretical studies consistently show that electron density moves from the pyrrole ring to the benzene ring during the transition.[16] Therefore, a positively charged environment around the benzene ring, or conversely, a negatively charged environment around the pyrrole ring, would reduce the transition energy, causing a red shift in the emission spectrum. This internal Stark effect depends only on the magnitude and sign of the electric field projected onto the indole ring and not the sources of the electric field. The effect of electrostatic environment on λ_{max} has been simulated using hybrid quantum mechanical/molecular dynamics (QM/MD) calculations, in which the electrostatic environment determined

* Authors to whom correspondence should be addressed. Phone: (406) 994-5414 (P.C.); (216) 368-0602 (M.B.). Fax: (406) 994-5407 (P.C.); (216) 368-0604 (M.B.). E-mail: pcallis@montana.edu; mdb4@case.edu.

[†] Case Western Reserve University.

[‡] Montana State University.

10.1021/jp056164p CCC: $33.50
Published on Web 03/16/2006

by molecular dynamics affects the transition energy determined by quantum mechanics by incorporating a modified Fock operator.[14,15] The simulated λ_{max} of 19 tryptophan residues in 16 proteins were in good agreement with the experimental values. Here, we report QM/MD simulations of the six canonical side chain rotamers of tryptophan in the seven cyclic hexapeptides. The results are consistent with differences in electrostatic environment among rotamers. The simulated λ_{max} are compared with the experimental λ_{max} of the DAS. Some new correlations between rotamer conformation and fluorescence lifetime are suggested by this approach.

2. Experimental Section

2.1. Time-Resolved Emission Spectroscopy. Peptide design and synthesis were described previously.[13] Fluorescence measurements were made on solutions of cyclic peptides in 0.01 M phosphate buffer, pH 6.9, as before.[13] Fluorescence decay curves were acquired using a time-correlated single photon counting instrument with a Spectra-Physics Tsunami mode-locked Ti: sapphire laser pumped by a Millennia diode-pumped Nd−YVO_4 laser.[13,18] The excitation wavelength was 300 nm; the emission wavelength was 325−400 nm. Time-resolved emission spectral data with $\geq 2 \times 10^4$ counts in the peak were acquired at 5 nm intervals with a 4 nm band-pass for experiments at 5 °C and at 10 nm intervals with an 8 nm band-pass for experiments at 25 °C. Decay data were stored in 1024 channels of 7.3, 9.8, and 24.4 ps per channel, corresponding to 7.5, 10, and 25 ns time scales. Decay curves were deconvolved using the Beechem global program,[19] assuming a sum of exponentials

$$I(\lambda,t) = \sum_i \alpha_i(\lambda) \exp(-t/\tau_i) \quad (1)$$

with amplitudes $\alpha_i(\lambda)$ at wavelength λ and lifetimes τ_i. The lifetimes, but not the amplitudes, were linked in the global analysis of decay data at different emission wavelengths. An additional component of 4−90 ps lifetime, representing the Raman scatter and stray light, was included in the analysis.[13] Goodness of fit was judged by reduced chi-square, χ_r^2, and the autocorrelation function of the weighted residuals.

Decay-associated emission spectra $F_i(\lambda)$ were constructed by combining the steady-state emission spectrum $F(\lambda)$ and the time-resolved emission spectral data

$$F_i(\lambda) = \alpha_i(\lambda)\tau_i F(\lambda) / \sum_i \alpha_i(\lambda)\tau_i \quad (2)$$

Smooth curves were drawn through the calculated points using the seventh-order polynomial fit in Origin (OriginLab), and λ_{max} values were read from the curves. For five peptides, two complete sets of time-resolved spectral data were collected, two sets of DAS were constructed, and average λ_{max} values were determined. The average deviations of ±0−2 nm in λ_{max} were within the 5 nm resolution of the time-resolved spectral data at 5 °C.

2.2. QM/MD Calculations. The wavelength of maximum emission was simulated as described.[14,15] Initial structures for the simulations were prepared from NMR structures of the cyclic peptides.[13] Six canonical rotamers of the tryptophan side chain were generated by setting $\chi_1 = \pm 60°$, 180° and $\chi_2 = \pm 90°$, followed by a 500 step conjugate gradient optimization with χ_1, χ_2 constrained. The $\chi_1 = -60°$ rotamers of the phosphotyrosine (pTyr, pY) side chain were generated similarly. The resulting structures were solvated with TIP3 model waters, and the energy was minimized with 1000 adapted basis Newton Raphson iterations, using a nonbonded interaction cutoff of 10 Å, no electrostatic cutoff, and a dielectric constant $\epsilon = 1$.[15] Solvated peptides were generated by superimposing a cube containing 8000 water molecules on the peptide structure, removing overlapping waters, and truncating the cube to a sphere of 25 Å radius. Peptides at the center of the water sphere were solvated to a depth of at least 17 Å. The phosphate group of phosphotyrosine was given a charge of −1 at neutral pH.

TABLE 1: Wavelengths of Maximum Emission for Steady-State Spectra and DAS[a]

peptide	sequence	$F(\lambda_{max})$ (nm)	$F_1(\lambda_{max})$ (nm)	$F_2(\lambda_{max})$ (nm)	$F_3(\lambda_{max})$ (nm)
2a	c[D-PWTFFpY]	353	355 ± 0	352 ± 0	341 ± 1
		355[b]	358[b]	354[b]	343[b]
2b	c[D-PWTpYFF]	354	354 ± 0	354 ± 0	342 ± 2
		355[b]	356[b]	354[b]	345[b]
3	c[D-PpYWTFF]	355	359 ± 0	353 ± 1	348 ± 1
4a	c[D-PpYTWFF]	351	356 ± 1	348 ± 2	341 ± 2
4b	c[D-PpYFWFT]	352	356	350	343
5	c[D-PpYTFWF]	350	351	341	346
6	c[D-PpYTFFW]	351	354 ± 1	351 ± 1	349 ± 1

[a] At 5 °C. Errors in $F_i(\lambda_{max})$ are average deviations from two DAS. [b] At 25 °C.

The QM calculations used Zerner's spectroscopically calibrated INDO/S method,[20] modified to allow input of electrostatic potentials and fields.[21,22] QM was used to assign charges to the indole ring and C_β. The transition energy calculation with added potentials and fields was performed on a 3-methylindole molecule in a reference ground- or excited-state geometry, using 196 singly excited configurations, Mataga−Nishimoto electron repulsion screening, and the original CNDO/S overlap factors. The MD calculations were done at 300 K on the solvated peptide, using CHARMM (version 26) with the CHARMM22 force field[23] and QM modified charges on the 3-methylindole part of tryptophan. The SHAKE constraint was applied to bonds in the indole ring.[24] The radius of the water sphere was constrained to 25 Å during the MD trajectory by a quartic potential. The trajectory was interrupted every 10 fs to perform an INDO/S−CIS calculation and update the tryptophan geometry and charges.

Tryptophan excitation was simulated by switching the geometry and charges of the 3-methylindole from the reference ground-state to the ^1L_a excited-state values. The geometry for the reference ground state came from a tryptophan crystal structure.[25] The geometry difference between ground and ^1L_a states came from an ab initio calculation.[26] Simulations started with 5 ps of ground-state dynamics, then switched the tryptophan geometry and charges to the ^1L_a state, and continued with 30 ps of excited-state dynamics. The λ_{max} values were calculated from the average transition energy over the excited-state trajectory. To minimize bias due to short-time relaxation effects, the first 10 ps of excited-state dynamics was omitted from the average. Decomposition of wavelength shifts into contributions from individual amino acid residues and water molecules was done using the previously described analysis tool.[15] Contributions from peptide structure and solvent are the sums of contributions from individual residues and waters.

3. Results

3.1. Emission Spectra. Table 1 gives the sequences of the cyclic hexapeptides. The peptide name denotes the position of the single tryptophan in the sequence. The cyclic peptides have triple-exponential fluorescence decays with lifetimes of $\tau_1 = 4.4-6.6$, $\tau_2 = 1.4-3.2$, and $\tau_3 = 0.2-1.0$ ns at 5 °C.[13] Table

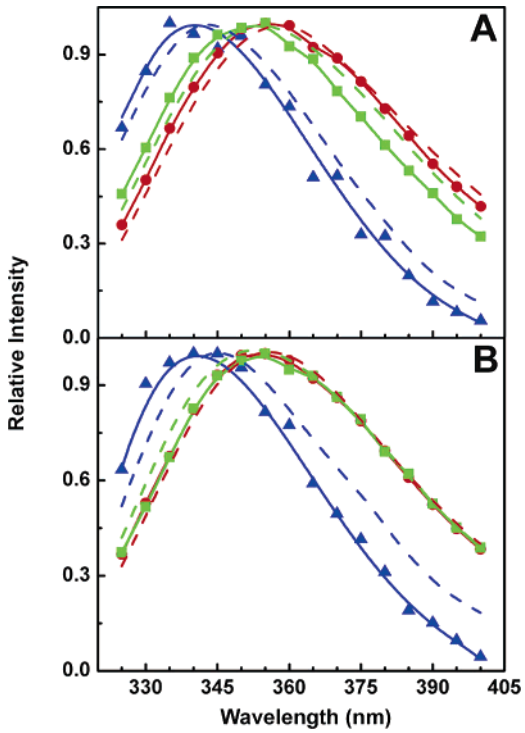

Figure 1. DAS of peptides **2a** and **2b** at 5 °C (solid lines) and 25 °C (dashed lines) normalized to peak intensity. (A) Peptide **2a**, $\tau_1 = 4.7$ ns (red), $\tau_2 = 2.8$ ns (green), and $\tau_3 = 0.8$ ns (blue) for 5 °C; $\tau_1 = 4.4$ ns (red), $\tau_2 = 2.8$ ns (green), and $\tau_3 = 0.7$ ns (blue) for 25 °C. (B) Peptide **2b**, $\tau_1 = 4.4$ ns (red), $\tau_2 = 2.4$ ns (green), and $\tau_3 = 1.0$ ns (blue) for 5 °C; $\tau_1 = 3.7$ ns (red), $\tau_2 = 2.3$ ns (green), and $\tau_3 = 0.6$ ns (blue) for 25 °C.

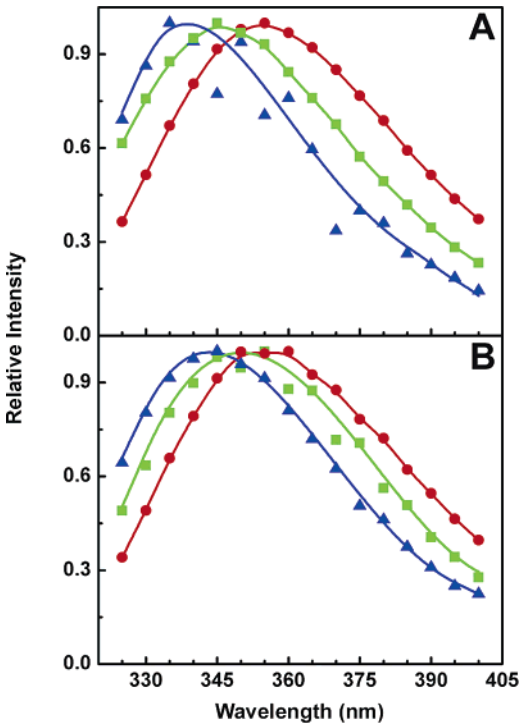

Figure 2. DAS of peptides **4a** and **4b** at 5 °C normalized to peak intensity. (A) Peptide **4a**, $\tau_1 = 6.6$ ns (red), $\tau_2 = 2.0$ ns (green), and $\tau_3 = 0.2$ ns (blue). (B) Peptide **4b**, $\tau_1 = 5.2$ ns (red), $\tau_2 = 2.0$ ns (green), and $\tau_3 = 0.5$ ns (blue).

1 summarizes the wavelengths of maximum emission of the steady-state and decay-associated emission spectra. While the steady-state emission maxima of the peptides vary only from 350 to 355 nm, the DAS emission maxima vary from 341 to 359 nm with a 5−15 nm range within a given peptide. The long-lifetime component, with emission maxima of DAS $F_1(\lambda)$ between 351 and 359 nm, has less spectral dispersion than the intermediate and short-lifetime components. Time-resolved emission spectroscopy clearly reveals additional details about the heterogeneous environment of tryptophan. The normalized DAS in Figures 1−3 illustrate the spectral shifts of the three lifetime components. Some of the DAS, for example, $F_1(\lambda)$ of peptide **2a** and $F_2(\lambda)$ of peptide **2b**, appear to have a shoulder, suggestive of two or more unresolved lifetime components with different emission spectra.

Peptides **2a** and **2b** have the single phosphotyrosine at positions 6 and 4 in the sequence. The backbone conformation of Trp[2] is about the same in both peptides,[13] providing an opportunity to examine the effects of distance between tryptophan and phosphotyrosine on the emission maxima. A phosphotyrosine at these two positions has a slight effect on the λ_{max} of the DAS (Table 1). For both peptides, the emission maxima of the short-lifetime DAS $F_3(\lambda)$ are 13−15 nm to the blue of the long- and intermediate-lifetime DAS $F_1(\lambda)$ and $F_2(\lambda)$. Peptide **2a** follows the common trend of a progressively red-shifted DAS with increasing lifetime, whereas peptide **2b** has two lifetime components with identical DAS (Figure 1). Increasing temperature from 5 to 25 °C results in small red shifts of the three DAS of peptide **2a** but only red-shifts the short-lifetime DAS $F_3(\lambda)$ of peptide **2b**.

Peptides **4a** and **4b** have the single threonine (Thr, T) at positions 3 and 6 in the sequence. The backbone conformation of Trp[4] is slightly different in the two peptides.[13] Both peptides show progressively red-shifted DAS with increasing lifetime, with the two long-lifetime DAS $F_1(\lambda)$ having almost the same λ_{max} (Figure 2). However, the intermediate- and short-lifetime DAS $F_2(\lambda)$ and $F_3(\lambda)$ lie 2 nm to the blue in peptide **4a** compared to those in peptide **4b**.

The DAS of peptides **3** and **6** shift progressively to the red as the lifetime increases (Figure 3). The spectral shifts are 5−6 nm for peptide **3** but only 2−3 nm for peptide **6**. In contrast, the intermediate-lifetime DAS $F_2(\lambda)$ of peptide **5** lies 5 nm to the blue of the short-lifetime DAS $F_3(\lambda)$. This wavelength dependence was not as obvious in previous time-resolved emission spectral data for peptide **5** using 10 nm intervals at 25 °C.[8] Presumably, the lower spectral resolution precluded observation of the small shifts.

3.2. Wavelength Calculations. In the standard rotamer model, different peptide conformers with different emission spectra would give rise to spectral heterogenity in the DAS. The peptides each have a single predominant backbone conformation with multiple side chain conformations of the solvent-exposed tryptophan.[13] Therefore, wavelength calculations were done for six canonical tryptophan rotamers of each peptide. Simulations of tryptophan in the ^1L_a excited state were run at 300 K according to the method used previously for proteins.[15] No restraints were applied to the tryptophan side chain. The structure was monitored every 100 fs throughout the MD trajectory. The χ_1, χ_2 angles of tryptophan fluctuated at most ±25° around the initial rotamer conformation. Emission maxima obtained from single trajectories are summarized in Table 2. The calculated λ_{max} values range from 344 to 365 nm with standard deviations of 10−15 nm (Table 2). The 20 nm range in calculated λ_{max} values of a solvent-exposed tryptophan in the peptides is surprising.

The precision of calculated λ_{max} values was evaluated by additional simulations on the two rotamers of peptide **3** with the most red- and blue-shifted emission maxima among the

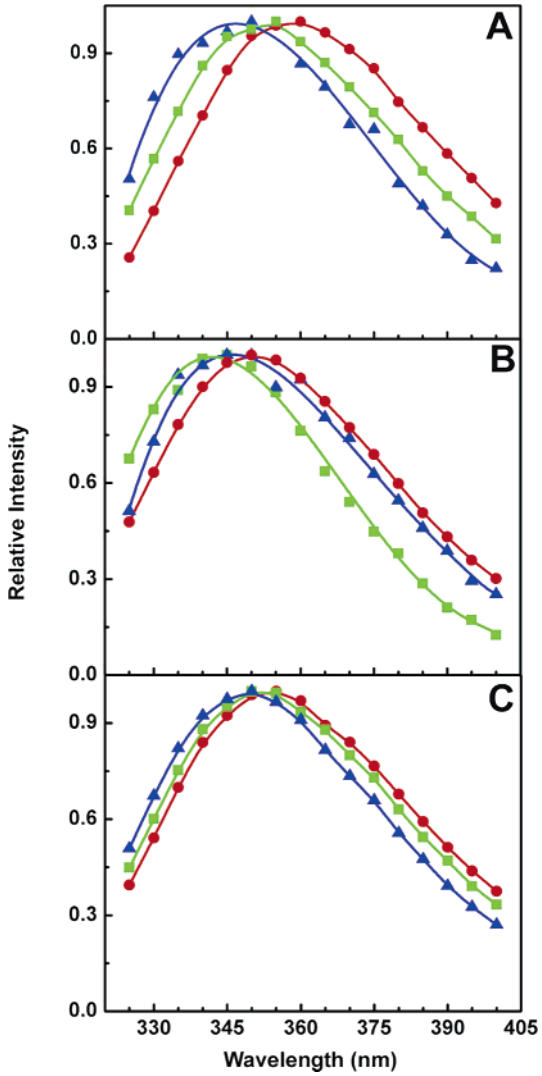

Figure 3. DAS of peptides **3**, **5**, and **6** at 5 °C normalized to peak intensity. (A) Peptide **3**, $\tau_1 = 6.0$ ns (red), $\tau_2 = 2.7$ ns (green), and $\tau_3 = 0.5$ ns (blue). (B) Peptide **5**, $\tau_1 = 5.5$ ns (red), $\tau_2 = 3.2$ ns (green), and $\tau_3 = 0.7$ ns (blue). (C) Peptide **6**, $\tau_1 = 4.9$ ns (red), $\tau_2 = 1.4$ ns (green), and $\tau_3 = 0.5$ ns (blue).

peptides, $(\chi_1, \chi_2) = (180°, -90°)$ and $(\chi_1, \chi_2) = (60°, -90°)$. Figure 4 shows a 60 ps dynamics trajectory for these rotamers. The large fluctuations of ground → ^1L_a transition energy are typical of all the peptide simulations as well as previous simulations of solvent-exposed tryptophans in proteins.[15] The λ_{max} values in Table 2 represent the 20 ps trajectory from 10 to 30 ps. The reproducibility of λ_{max} was estimated from the average transition energy of 20 ps trajectories in other regions of the simulation. The values from four 20 ps trajectories starting at 10−40 ps in 10 ps intervals varied from 4 to 6 nm with an average λ_{max} of 363 ± 2 nm for the $(\chi_1, \chi_2) = (180°, -90°)$ rotamer and 344 ± 3 nm for the $(\chi_1, \chi_2) = (60°, -90°)$ rotamer (Table 3). The effect of simulation temperature on λ_{max} was determined, because the DAS λ_{max} in Table 1 were measured at 5 °C and the calculated λ_{max} in Table 2 were simulated at 27 °C. Simulations run on the two rotamers at 278 K gave λ_{max} values within the range of values obtained at 300 K (Table 3). For solvent-exposed tryptophans, the initial positioning of solvent molecules in the calculation may affect the calculated λ_{max} values. Solvation effects were examined by shifting the peptide coordinates 0.5 Å along the *x*- or *y*-axis before adding the water. The λ_{max} values from four solvation conditions varied from 6 to 12 nm with an average λ_{max} of 359 ± 3 nm for the

TABLE 2: Calculated Wavelengths of Maximum Emission in nm for Tryptophan Rotamers

	$\chi_1 = -60°$		$\chi_1 = 180°$		$\chi_1 = 60°$	
peptide[a]	$\chi_2 = -90°$	$\chi_2 = 90°$	$\chi_2 = -90°$	$\chi_2 = 90°$	$\chi_2 = -90°$	$\chi_2 = 90°$
2a[b]	354 ± 11	361 ± 13	352 ± 11	358 ± 13	357 ± 13	362 ± 13
2a*[c]	359 ± 13	356 ± 12	354 ± 12	356 ± 12	354 ± 11	348 ± 11
2a(Y)[b]	359 ± 14	361 ± 13	354 ± 12	355 ± 11	347 ± 12	351 ± 11
2b[b]	362 ± 12	356 ± 13	352 ± 11	351 ± 12	349 ± 12	347 ± 10
2b(Y)[b]	358 ± 11	355 ± 12	350 ± 10	356 ± 12	355 ± 12	345 ± 12
3[b]	353 ± 11	358 ± 13	365 ± 12	351 ± 11	344 ± 10	359 ± 15
3*[c]	351 ± 11	349 ± 13	350 ± 15	352 ± 11	360 ± 11	344 ± 10
3(Y)[b]	357 ± 12	346 ± 12	354 ± 11	357 ± 11	361 ± 11	345 ± 12
4a[b]	356 ± 12	354 ± 12	348 ± 11	355 ± 11	349 ± 12	349 ± 12
4a(Y)[b]	356 ± 12	358 ± 12	351 ± 11	346 ± 12	353 ± 11	349 ± 12
4b[c]	351 ± 12	354 ± 12	346 ± 12	351 ± 11	344 ± 10	352 ± 11
4b(Y)[c]	362 ± 12	356 ± 12	351 ± 11	353 ± 13	352 ± 11	348 ± 11
5[c]	358 ± 13	357 ± 13	352 ± 11	355 ± 13	353 ± 12	348 ± 11
5(Y)[c]	356 ± 11	358 ± 12	352 ± 12	354 ± 13	356 ± 11	353 ± 12
6[b]	354 ± 12	360 ± 13	353 ± 11	353 ± 11	360 ± 13	356 ± 13
6(Y)[b]	359 ± 13	355 ± 12	353 ± 12	350 ± 11	356 ± 12	351 ± 11

[a] Y denotes a peptide with phosphotyrosine replaced by tyrosine; an asterisk denotes a peptide with a different pY side chain rotamer. [b] pY side chain rotamer was $\chi_1 = 180°$. [c] pY side chain rotamer was $\chi_1 = -60°$.

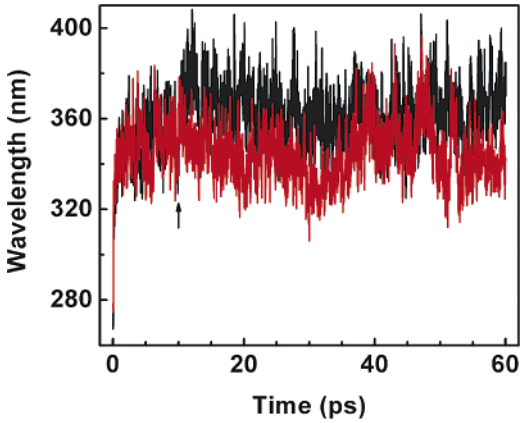

Figure 4. Plot of calculated transition wavelength versus time during the dynamics trajectories of two Trp^3 rotamers of peptide **3**: $(\chi_1, \chi_2) = 180°, -90°$ rotamer (black) and $(\chi_1, \chi_2) = 60°, -90°$ rotamer (red).

$(\chi_1, \chi_2) = (180°, -90°)$ rotamer and 351 ± 5 nm for the $(\chi_1, \chi_2) = (60°, -90°)$ rotamer (Table 3). The overall average of λ_{max} values from the different simulation protocols in Table 3 are 361 ± 3 nm for the $(\chi_1, \chi_2) = (180°, -90°)$ rotamer and 348 ± 5 nm for the $(\chi_1, \chi_2) = (60°, -90°)$ rotamer. Thus, the uncertainty in calculated λ_{max} values appears to be about 3−5 nm, with blue-shifted emission maxima being perhaps somewhat less certain.

Figure 5 shows the estimated decomposition of the spectral shifts, relative to vacuum, into contributions from peptide and water molecules. The peptide contribution comprises the contributions from all other residues plus the tryptophan backbone. Positive values are shifts to longer wavelengths; negative values are shifts to shorter wavelengths. The sum of the peptide and water contributions defines the net spectral shift given in Table 2. In all peptides, the total water contribution causes a red shift of 13−67 nm. In a previous simulation of the λ_{max} of *Staphylococcus* nuclease, waters near W140 contributed a large blue shift primarily by forming chains with two red-shifting lysines close to the benzene ring of indole.[15] Blue-shifting waters are found in the peptide trajectories. These waters

TABLE 3: Effect of Simulation Conditions on Calculated Wavelengths for Two Rotamers of Peptide 3

	λ_{max} (nm)				
condition	10−30 ps	20−40 ps	30−50 ps	40−60 ps	10−60 ps
	$\chi_1 = 180°, \chi_2 = -90°$				
300 K	365 ± 12	361 ± 11	361 ± 12	363 ± 13	364 ± 12
278 K	362 ± 14				
0.5 Å *x*-axis shift[a]	362 ± 12				
~0.15 Å *x*-axis shift[b]	356 ± 12				
0.5 Å *y*-axis shift[a]	358 ± 12				
~0.15 Å *y*-axis shift[b]	358 ± 12				
	$\chi_1 = 60°, \chi_2 = -90°$				
300 K	344 ± 10	341 ± 12	347 ± 14	346 ± 13	344 ± 12
278 K	347 ± 10				
0.5 Å *x*-axis shift[a]	352 ± 12				
~0.15 Å *x*-axis shift[b]	345 ± 11				
0.5 Å *y*-axis shift[a]	357 ± 13				
~0.15 Å *y*-axis shift[b]	350 ± 11				

[a] 0.5 Å coordinate shift performed by CHARMM. [b] 0.5 Å coordinate shift performed manually.

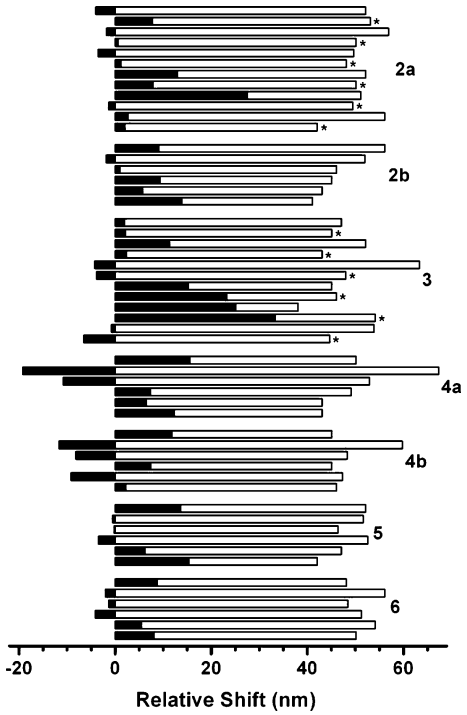

Figure 5. Estimated contribution to tryptophan spectral shift from peptide (solid bars) and water (open bars) molecules. For each peptide, Trp rotamers from top to bottom are (i, i*) (χ_1, χ_2) = −60°, −90°; (ii, ii*) (χ_1, χ_2) = −60°, 90°; (iii, iii*) (χ_1, χ_2) = 180°, −90°; (iv, iv*) (χ_1, χ_2) = 180°, 90°; (v, v*) (χ_1, χ_2) = 60°, −90°; (vi, vi*) (χ_1, χ_2) = 60°, 90°. Positive values are red shifts, and negative values are blue shifts relative to vacuum. The pTyr rotamer is $\chi_1 = 180°$ for peptides **2a** and **3**; $\chi_1 = -60°$ for peptides **2a*** and **3***. See Table 2 and text for details.

point oxygen to the benzene ring or hydrogen to the pyrrole ring or form short chains. However, the waters maintain these geometries only transiently and thereby contribute negligibly to the excited-state energy.

The total peptide contribution varies in magnitude from 1 to 33 nm with blue shifts as large as −19 nm or red shifts as large as +33 nm, depending on the peptide as well as side chain rotamer. The peptide and water contributions to the spectral shifts of the seven peptides are strongly anticorrelated (Figure 6). However, neither peptide nor water contributions correlate with the spectral shift. A similar anticorrelation between peptide and water contributions is found for proteins, which is weaker for buried than exposed tryptophans.[15] For solvent-exposed

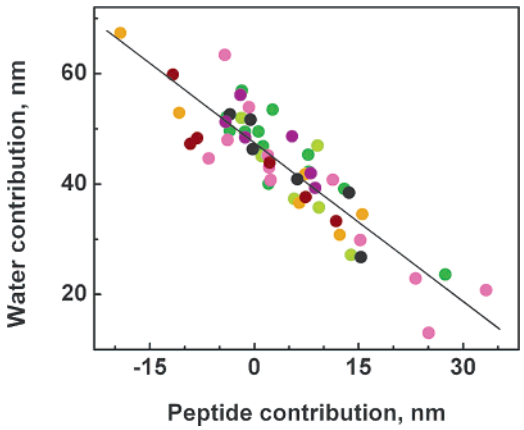

Figure 6. Plot of water versus peptide contributions to tryptophan spectral shifts of the six χ_1, χ_2 rotamers in peptide **2a**, **2a*** (green), **2b** (yellow-green), **3**, **3*** (magenta), **4a** (tan), **4b** (brown), **5** (black), and **6** (purple) from Figure 5. The black line is the least-squares fit to water = −1.05 protein + 60; correlation coefficient $R = -0.93$.

tryptophans in peptides and proteins, the large anticorrelation with the water contribution reflects the dielectric constant of water, even though it is not put explicitly into the calculations.

The peptide sequences contain three residues with nonpolar side chains, which should not have much effect on the peptide contribution to the electrostatic environment of the indole ring. The polar peptide backbone should account for most of the peptide contribution to the spectral shift, primarily the two peptide bonds on either side of the tryptophan. Figure 7 shows the contributions from individual residues of each peptide with tryptophan at position *i* in the sequence. Tryptophan rotamer conformations are illustrated by Newman projections along the $C_i^{\alpha}-C_i^{\beta}$ bond in each panel. The peptide contribution for amino acids other than tryptophan includes side chain as well as backbone atoms. For the $\chi_1 = -60°$ rotamers, the proximate polar group to the indole is the peptide bond between tryptophan and the preceding residue, which comprises the CO of residue $(i - 1)$ and the NH of residue *i*. Thus, residues $(i - 1)$ and *i* are expected to make a larger contribution to the shift. Panels A and D demonstrate this trend with mainly red shifts for $\chi_2 = -90°$ rotamers and blue shifts for $\chi_2 = 90°$ rotamers. For the $\chi_1 = 180°$ rotamers, the proximate peptide bond is between tryptophan and the following residue. Panels B and E show a tendency for larger contributions from residue *i* for $\chi_2 = -90°$ rotamers and residue $(i + 1)$ for $\chi_2 = 90°$ rotamers. For $\chi_1 = 60°$ rotamers, the peptide bonds on both sides of tryptophan are close to the indole ring. While the $\chi_2 = -90°$ rotamer (panel C) shows some larger contributions from residue *i*, the $\chi_2 = 90°$ rotamer (panel F) has no trends in the spectral shift.

As noted previously, charged side chains can make significant contributions to the spectral shifts in proteins.[15] A phosphotyrosine residue was designed into the peptide sequence to increase solubility in aqueous solution. To examine the effect of the phosphate group, simulations were carried out on seven peptides, in which phosphotyrosine was mutated to tyrosine in silico (Table 2). The resulting changes in λ_{max} are quite variable, ranging from no shift to red or blue shifts as large as 17 nm, depending on peptide sequence and rotamer. In peptide **3** with Trp^3 sandwiched between $pTyr^2$ and Thr^4 on one side of the cyclic backbone, three rotamers have large blue shifts, one rotamer has a large red shift, and the other two rotamers have modest red shifts. In contrast, in peptide **4a** with Trp^4 following $pTyr^2$ and Thr^3, one rotamer has a large blue shift and the other rotamers have negligible if any shifts. These results suggest that

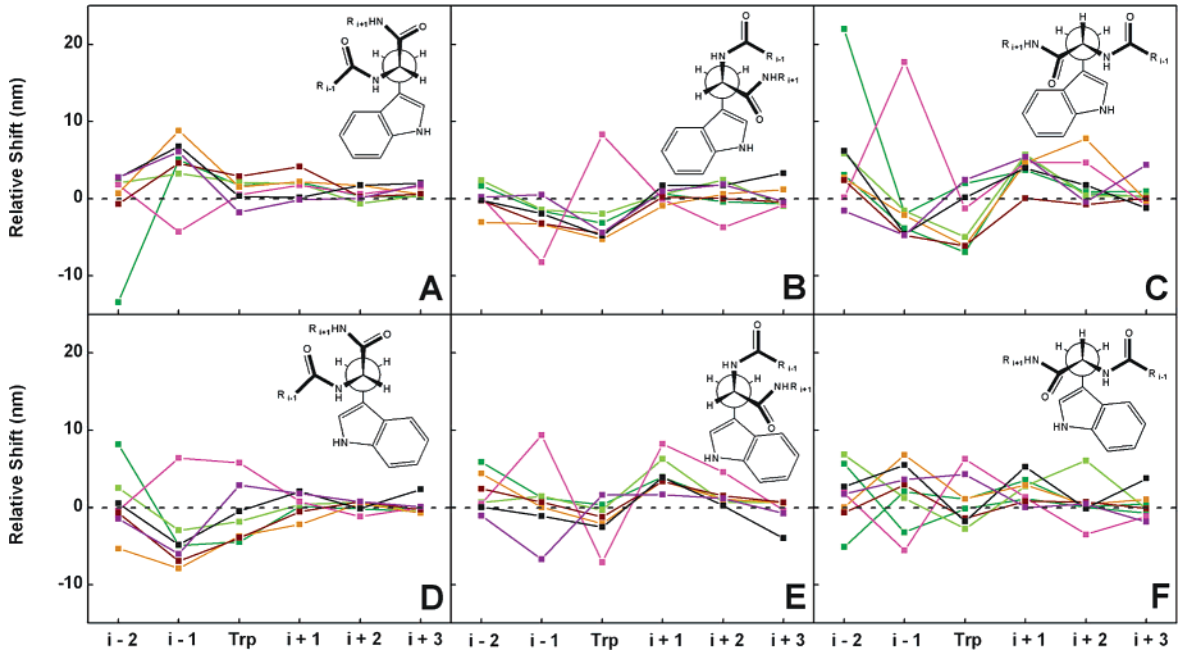

Figure 7. Estimated peptide contribution to tryptophan spectral shift from each residue in peptide **2a** (green), **2b** (yellow-green), **3** (magenta), **4a** (tan), **4b** (brown), **5** (black), and **6** (purple). Trp rotamers: (A) (χ_1, χ_2) = −60°, −90°; (B) (χ_1, χ_2) = 180°, −90°; (C) (χ_1, χ_2) = 60°, −90°; (D) (χ_1, χ_2) = −60°, 90°; (E) (χ_1, χ_2) = 180°, 90°; (F) (χ_1, χ_2) = 60°, 90°. Positive values are red shifts, and negative values are blue shifts relative to vacuum.

TABLE 4: Phosphotyrosine Side Chain Conformations from NMR Data, 5 °C[a]

peptide	average structure	$^3J_{H\alpha-H\beta r}$[b] (Hz)	$^3J_{H\alpha-H\beta s}$[b] (Hz)	pI[c]	major rotamer	pII[c]	pIII[c]
2a	$\chi_1 = 180°$	8.5	4.8	0.59	$\chi_1 = -60°$	0.25	0.16
2b	$\chi_1 = 180°$	8.3	7.3	0.52	$\chi_1 = 180°$	0.43	0.05
3	$\chi_1 = 180°$	9.2	5.4	0.60	$\chi_1 = -60°$	0.26	0.14
4a	$\chi_1 = 180°$	10.3	4.3	0.70	$\chi_1 = -60°$	0.16	0.14
4b	$\chi_1 = -60°$	11.3	4.4	0.79	$\chi_1 = -60°$	0.16	0.05
5	$\chi_1 = -60°$	10.2	4.8	0.70	$\chi_1 = -60°$	0.19	0.11
6	$\chi_1 = 180°$	10.7	4.0	0.74	$\chi_1 = -60°$	0.14	0.12

[a] Reference 13. [b] Coupling constants. [c] χ_1 rotamer populations.

the conformation of the phosphotyrosine side chain may influence the λ_{max} value.

Like tryptophan, phosphotyrosine adopts multiple side chain conformations in solution. Table 4 gives the χ_1 rotamer populations of the phosphotyrosine side chain determined from the previously reported NMR data for the peptides.[13] The major pTyr rotamer is $\chi_1 = 180°$ for peptide **2b** and $\chi_1 = -60°$ for the other six peptides. In the average NMR structures used for the simulations, the phosphotyrosine side chain ends up in the $\chi_1 = -60°$ rotamer conformation in peptides **4b** and **5** and the $\chi_1 = 180°$ rotamer conformation in the other five peptides (Table 4). To test the effect of phosphotyrosine orientation on the electrostatic environment of the indole ring, simulations were performed on peptides **2a** and **3** with phosphotyrosine in the $\chi_1 = -60°$ conformation. Like tyrosine substitution, the effects of phosphotyrosine orientation on simulated λ_{max} values are variable (Table 2). As evident in Figure 5, phosphotyrosine orientation can have appreciable effects on both peptide and water contributions to the spectral shift.

Figure 8 shows the two $\chi_1 = 60°$ Trp rotamers of peptide **2a** with two conformations of the phosphotyrosine side chain. For the (χ_1, χ_2) = 60°, −90° Trp rotamer, the phosphate group is near and almost coplanar, with the indole ring closer to the pyrrole ring in the $\chi_1 = 180°$ pTyr rotamer (left side). This position is consistent with the huge red shift in the peptide contribution to the spectral shift (Figure 5). The phosphate is

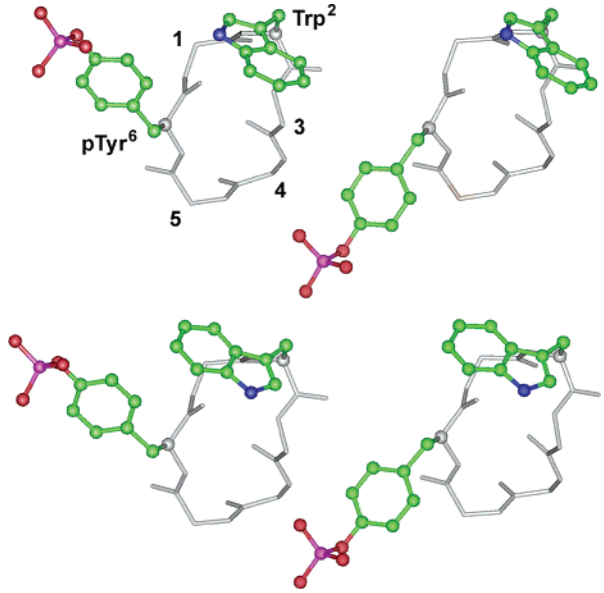

Figure 8. Structures of peptide **2a** showing two rotamer conformations of Trp^2 and pTyr^6. Top: (χ_1, χ_2) = 60°, −90° rotamer of Trp^2, χ_1 = 180° rotamer of pTyr^6 (left side) and $\chi_1 = -60°$ rotamer of pTyr^6 (right side). Bottom: (χ_1, χ_2) = 60°, 90° rotamer of Trp^2, $\chi_1 = 180°$ rotamer of pTyr^6 (left side) and $\chi_1 = -60°$ rotamer of pTyr^6 (right side).

farther away and lies between the pyrrole and the benzene rings in the $\chi_1 = -60°$ pTyr rotamer (right side), which has a small blue shift in the peptide contribution. However, these large differences in peptide contribution are masked by anticorrelation with the water contribution, so that the net effect of phosphate orientation on the λ_{max} values of the (χ_1, χ_2) = 60°, −90° Trp rotamer is only 3 nm (Table 2). By contrast, for the (χ_1, χ_2) = 60°, 90° Trp rotamer, the phosphate group is near but out of plane of the indole ring about equidistant from the pyrrole and benzene rings in the $\chi_1 = 180°$ pTyr rotamer (left side), which has a small red shift in the peptide contribution. In the $\chi_1 = -60°$ pTyr rotamer (right side), which also has a small red shift

in the peptide contribution, the phosphate is positioned similarly to the (χ_1, χ_2) = 60°, −90° Trp rotamer. In this case, despite similar small red shifts in the peptide contribution, a larger difference in the water contributions causes a 14 nm effect of the phosphate group on the λ_{max} values of the (χ_1, χ_2) = 60°, 90° Trp rotamer.

4. Discussion

The strong correlation of DAS λ_{max} and fluorescence lifetime commonly observed in proteins is manifest in five of the seven cyclic hexapeptides. Although this correlation is not presently understood, it is clearly dictated by an underlying physical principle. The absence of plausible hypotheses for the nature of this principle is used as evidence against the standard rotamer model. Relaxation models, in contrast, naturally predict this correlation. However, excited-state reactions require negative amplitudes in the decay kinetics. These were not observed in the cyclic peptides[13] and are very rarely seen in proteins.[27] The simulation results presented here speak only to the existence of a rationale for a substantial dependence of λ_{max} on rotamer conformation, a requirement for the validity of any rotamer-based mechanism. A single rotamer of the solvent-exposed tryptophan in the cyclic peptides is not expected to exhibit excited-state heterogeneity due to dielectric relaxation of solvent alone in response to the excitation-induced dipole change, a process that experimentally is known to have a time constant of 1.2 ps.[28]

Previous NMR studies showed substantial populations of three χ_1 rotamers in six of the seven cyclic peptides and suggested little χ_2 preference in any peptide.[13] No attempt was made here to assess the equilibrium rotamer populations with MD simulations, because the parametrization is probably not accurate enough. However, a number of computational studies have explored the energy surfaces of tryptophan,[29,30] *N*-acetyltryptophanamide,[31,32] and *N*-acetyltryptophan methylamide (NATMA).[31−33] These ab initio calculations correctly predicted the most stable conformers observed in cold expansion jets.[29−33] The study by Bombasaro et al. using B3LYP/6-31g* found 34 stable conformers.[33] Such computations are not directly applicable to our work, because the cyclic peptide backbone adopts conformations that do not arise for NATMA naturally and because the calculations do not model solvation realistically. However, the relative energies of various rotamers may be representative. Interestingly, the ab initio result predicts that only three rotamers with population >10% would occur at 5 °C.[33] For the α_L-helix backbone conformation, only three stable rotamers were found with a dominant one representing 96% of the population.

For the solvent-exposed tryptophan in the cyclic peptides, the calculated λ_{max} values from 20 ps trajectories have standard deviations of ±10−15 nm. Uncertainty in the calculated λ_{max} due to the simulation protocol is ±3−5 nm. Previous simulations for proteins gave calculated wavelengths within ±6 nm of the experimental values.[15] For the peptides, comparison between calculated and experimental wavelengths is less straightforward. First, the simulations give calculated λ_{max} for six χ_1, χ_2 rotamers of the tryptophan side chain, whereas the DAS give only three λ_{max} values. The average deviations in DAS λ_{max} values determined from time-resolved spectral data are about ±2 nm. Although the lifetime data are fitted with a fourth decay component to account for stray light, the λ_{max} values of 341−342 nm may have larger errors due to Raman scattering at 337 nm. Presumably, the three DAS represent the three χ_1 rotamers of the tryptophan side chain. While ^{1}H NMR data indicate the presence of six χ_1, χ_2 tryptophan rotamers in solution, these data can only determine the populations of the three χ_1 rotamers and identify a major χ_1 rotamer in those cases where one predominates.[13] The major χ_1 rotamer can be assigned to the DAS λ_{max} of the major lifetime component, assuming that the χ_2 rotamers do not generate lifetime heterogeneity. The association of χ_1 rotamer and DAS λ_{max} of the other two lifetime components is unknown. Of course, the relationship between rotamers and DAS λ_{max} would be more complicated if the lifetimes and emission spectra of the χ_2 rotamers of a given χ_1 rotamer differ significantly. Second, the simulations are performed on a single peptide structure with a single rotamer of each amino acid side chain, whereas the fluorescence lifetimes are measured on an ensemble of structures with multiple rotamers of each side chain. The calculated wavelengths in Table 2 are based on single trajectories. A few simulations on peptides **2a** and **3** for two χ_1 rotamers of phosphotyrosine show that the side chain conformation of other residues may significantly affect the calculated λ_{max}.

The above caveats limit comparison of calculated and experimental λ_{max} values to general trends. Both simulations and experiment give a 20 nm range in λ_{max} values for the peptides: 344−365 nm for calculated λ_{max} and 341−359 nm for DAS λ_{max}. Peptide **6** showed the least wavelength dispersion: 353−360 nm for calculated λ_{max} and 349−354 nm for DAS λ_{max}. The other peptides showed greater wavelength dispersion with reasonable agreement between calculated and experimental wavelength ranges. In previous studies, the major lifetime component was assigned to the major NMR-determined χ_1 rotamer assuming (1) only one major χ_2 rotamer, (2) fast interconversion between χ_2 rotamers, or (3) two χ_2 rotamers with similar lifetimes.[8,13] Inspection of Table 2 suggests that within error the χ_2 = ±90° rotamers have the same calculated λ_{max} values, except in the case of peptide **3**. For the major χ_1 rotamer, the calculated λ_{max} is generally consistent with the DAS λ_{max}. For peptides **2a**, **2b**, **4b**, and **5**, the major lifetime component with the most red-shifted DAS $F_1(\lambda_{max})$ was assigned to the χ_1 = −60° rotamer. The calculated λ_{max} for the χ_1 = −60°, χ_2 = ±90° rotamers in these peptides are red-shifted somewhat relative to the other rotamers. For peptide **3**, the major lifetime component with the intermediate DAS $F_2(\lambda_{max})$ was assigned to the χ_1 = −60° rotamer. Although peptide **3** is admittedly a special case, because of the extreme sensitivity to phosphotyrosine side chain conformation, the calculated λ_{max} values of 353 and 358 nm for the χ_1 = −60°, χ_2 = ±90° rotamers are intermediate to the extremes of 365 and 344 nm. Finally, for peptide **6**, the major lifetime component with the most blue-shifted DAS $F_3(\lambda_{max})$ was assigned to the χ_1 = 180° rotamer. The calculated λ_{max} for the χ_1 = 180°, χ_2 = ±90° rotamers in this peptide is blue-shifted somewhat relative to the other rotamers.

Some calculated λ_{max} values of χ_2 rotamers of a given χ_1 rotamer are quite different, notably the χ_1 = 180° and 60° rotamers of peptide **3** (Table 2). This indicates that the two χ_2 tryptophan rotamers have different electrostatic environments, arising from the adjacent, charged phosphotyrosine side chain as discussed above. If the calculated wavelength dispersion among χ_2 rotamers were real and accompanied by differences in fluorescence lifetime, then the three DAS might represent some combination of χ_2 = ±90° rotamers of the three χ_1 rotamers rather than simply the three χ_1 rotamers. A question then arises about the utility of wavelength calculations in correlating lifetime components and DAS with rotamers. Proceeding cautiously and sticking with the assumption that the DAS represent χ_1 rotamers, the calculated λ_{max} do not identify additional correlations for peptides **2a**, **3**, **4b**, and **6**. However,

they do suggest some correlations for peptides **2b**, **4a**, and **5**. Although the calculated λ_{max} values for the $\chi_1 = 180°$ and 60° rotamers of peptide **2b** are the same within error, the trend is consistent with $F_2(\lambda_{max})$ being the $\chi_1 = 180°$ rotamer and $F_3(\lambda_{max})$ being the $\chi_1 = 60°$ rotamer. In the case of peptide **4a**, the NMR-determined χ_1 rotamer populations were all equal, which foiled identification of a major rotamer and correlation with a lifetime component and DAS. However, the calculated λ_{max} indicate that the DAS $F_1(\lambda_{max})$ is the $\chi_1 = -60°$ rotamer. Last, for peptide **5**, the wavelength calculations point to $F_2(\lambda_{max})$ as the $\chi_1 = 60°$ rotamer and $F_3(\lambda_{max})$ as the $\chi_1 = 180°$ rotamer.

In summary, both calculated and experimental λ_{max} values of the cyclic peptides show that side chain rotamers can generate up to 20 nm wavelength dispersion for solvent-exposed tryptophans. Not surprisingly, water molecules make a major contribution to this wavelength dispersion. Comparison of calculated and experimental wavelengths is consistent with the rotamer model. Although a simple assumption that the DAS λ_{max} represent χ_1 rotamers is adequate in most cases, more elaborate scenarios including χ_2 rotamers are also possible. For single trajectories, uncertainty in calculated λ_{max} values precludes discrimination between alternative versions of the rotamer model as well as other explanations for the lifetime heterogeneity and wavelength dispersion in these peptides. Multiple runs under different simulation protocols would increase the precision of the calculated wavelengths.

Acknowledgment. Supported in part by National Science Foundation grant MCB-0133064 to P.R.C.

References and Notes

(1) Eftink, M. R. Intrinsic fluorescence of proteins. In *Protein Fluorescence*; Lakowicz, J. R., Ed.; Topics in Fluorescence Spectroscopy 6; Kluwer Academic/Plenum: New York, 2000; pp 1−15.
(2) Hudson, B. S.; Huston, J. M.; Soto-Campos, G. *J. Phys. Chem. A* **1999**, *103*, 2227−2234.
(3) Ladokhin, A. S. *J. Fluoresc.* **1999**, *9*, 1−9.
(4) Lakowicz, J. R. *Photochem. Photobiol.* **2000**, *72*, 421−437.
(5) Donzel, B.; Gaudchon, P.; Wahl, P. *J. Am. Chem. Soc.* **1974**, *96*, 801−808.
(6) Ross, J. B. A.; Rousslang, K. W.; Brand, L. *Biochemistry* **1981**, *20*, 4361−4369.
(7) Ross, J. B. A.; Wyssbrod, H. R.; Porter, R. A.; Schwartz, G. P.; Michaels, C. A.; Laws, W. R. *Biochemistry* **1992**, *31*, 1585−1594.
(8) Adams, P. D.; Chen, Y.; Ma, K.; Zagorski, M. G.; Sönnichsen, F. D.; McLaughlin, M. L.; Barkley, M. D. *J. Am. Chem. Soc.* **2002**, *124*, 9278−9286.
(9) Sillen, A.; Diaz, J. F.; Engelborghs, Y. *Protein Sci.* **2000**, *9*, 158−169.
(10) Hellings, M.; De Maeyer, M.; Verheyden, S.; Hao, Q.; Van Damme, E. J. M.; Peumans, W. J.; Engelborghs, Y. *Biophys. J.* **2003**, *85*, 1894−1902.
(11) Dahms, T. E. S.; Willis, K. J.; Szabo, A. G. *J. Am. Chem. Soc.* **1995**, *117*, 2321−2326.
(12) Clayton, A. H.; Sawyer, W. H. *Biophys. J.* **1999**, *76*, 3235−3242.
(13) Pan, C.-P.; Barkley, M. D. *Biophys. J.* **2004**, *86*, 3828−3835.
(14) Callis, P. R.; Burgess, B. K. *J. Phys. Chem. B* **1997**, *101*, 9429−9432.
(15) Vivian, J. T.; Callis, P. R. *Biophys. J.* **2001**, *80*, 2093−2109.
(16) Callis, P. R. *Methods Enzymol.* **1997**, *278*, 113−151.
(17) Pierce, D. W.; Boxer, S. G. *Biophys. J.* **1995**, *68*, 1583−1591.
(18) Zawadzki, K. M.; Pan, C.-P.; Barkley, M. D.; Johnson, D.; Taylor, S. S. *Proteins: Struct., Funct., Genet.* **2003**, *51*, 552.
(19) Beechem, J. M. *Chem. Phys. Lipids* **1989**, *50*, 237.
(20) Ridley, J.; Zerner, M. *Theor. Chim. Acta* **1973**, *32*, 111−134.
(21) Theiste, D.; Callis, P. R.; Woody, R. W. *J. Am. Chem. Soc.* **1991**, *113*, 3260−3267.
(22) Sreerama, N.; Woody, R. W.; Callis, P. R. *J. Phys. Chem.* **1994**, *98*, 10397−10407.
(23) MacKerell, A. D., Jr.; Bashford, D.; Bellott, M.; Dunbrack, R. L.; Evanseck, J. D.; Fields, M. J.; Fischer, S.; Gao, J.; Ha, S.; Joseph-McCarthy, D.; Kuchnir, L.; Kuczera, K.; Lau, F. T. K.; Mattos, C.; Michnick, S.; Ngo, T.; Nguyen, D. T.; Prodhom, B.; Reiher, W. E., III.; Roux, B.; Schlenkrich, M.; Smith, J. S.; Stote, R.; Straub, J.; Watanabe, M.; Wiorkiewicz-Kuczera, J.; Yin, D.; Karplus, M. *J. Phys. Chem. B* **1998**, *102*.
(24) Ryckaert, J. P.; Cicotti, G.; Berendsen, H. J. C. *J. Comput. Phys.* **1977**, *23*.
(25) Takigawa, T.; Ashida, T.; Sasada, Y.; Kakudo, M. *Bull. Chem. Soc. Jpn.* **1966**, *39*, 2369−2378.
(26) Callis, P. R.; Vivian, J. T.; Slater, L. S. *Chem. Phys. Lett.* **1995**, *244*, 53.
(27) Toptygin, D.; Savtchenko, R. S.; Meadow, N. D.; Brand, L. *J. Phys. Chem. B* **2001**, *105*, 2043−2055.
(28) Shen, X.; Knutson, J. R. *J. Phys. Chem. B* **2001**, *105*, 6260−6265.
(29) Compagnon, I.; Hagemeister, F. C.; Antoine, R.; Rayne, D.; Broyer, M.; Dugourd, P.; Hudgins, R. R.; Jarrold, M. F. *J. Am. Chem. Soc.* **2001**, *123*, 8440−8441.
(30) Huang, Z.; Lin, Z. *J. Phys. Chem. A* **2005**, *109*, 2656−2659.
(31) Dian, B. C.; Longarte, A.; Mercier, S.; Evans, D. A.; Wales, D. J.; Zwier, T. S. *J. Chem. Phys.* **2002**, *117*, 10688−10702.
(32) Dian, B. C.; Longarte, A.; Winter, P. R.; Zwier, T. S. *J. Chem. Phys.* **2004**, *120*, 133−147.
(33) Bombasaro, J. A.; Rodríguez, A. M.; Enriz, R. D. *THEOCHEM* **2005**, *724*, 173−184.